RSC Advances

This article can be cited before page numbers have been issued, to do this please use: A. Gutiérrez, F. Gutierrez, M. Eguílaz, J. M. Gonzalez-Dominguez, J. Hernandez, A. Ansón, M. T. Martínez and G. A. Rivas, *RSC Adv.*, 2016, DOI: 10.1039/C5RA22556F.

ROYAL SOCIETY OF CHEMISTRY

www.rsc.org/advances

View Article Online
DOI: 10.1039/C5RA22556F

RCS Advances

ARTICLE

Received 00th January 20xx,
Accepted 00th January 20xx

DOI: 10.1039/x0xx00000x

www.rsc.org/

Electrochemical sensing of guanine, adenine and 8-hydroxy-2'-deoxyguanosine at glassy carbon modified with single-walled carbon nanotubes covalently functionalized with lysine

Alejandro Gutiérrez[a], Fabiana A. Gutiérrez[a], Marcos Eguílaz[a], José M. González-Domínguez[b,c] , Javier Hernández-Ferrer[b], Alejandro Ansón-Casaos[b], María T. Martínez[b,*] and Gustavo A. Rivas[a,*]

This work reports the synthesis and characterization of single-walled carbon nanotubes (SWCNT) covalently functionalized with L-lysine (Lys) and the analytical performance of glassy carbon electrodes (GCE) modified with the dispersion (GCE/SWCNT-Lys) for the highly sensitive quantification of guanine, adenine and 8-hydroxy, 2´-deoxyguanosine. Detection limits of 75, 195 and 97 nM were obtained for guanine, adenine and 8-hydroxy-2´,deoxyguanosine, respectively by voltammetric adsorptive stripping with medium exchange. GCE/SWCNT-Lys was successfully used for the detection of adenine and guanine oxidation after adsorption of sperm double stranded DNA. A clear definition of 8-hydroxy-2´,deoxyguanosine oxidation signal is observed even in the presence of large excess of guanine, adenine or sperm-double stranded DNA.

1. Introduction

Carbon nanotubes (CNTs) have received enormous attention for the development of electrochemical (bio)sensors due to their fascinating properties, connected with a large surface-to-volume ratio, high mechanical strength, fast electron transfer kinetics, high chemical and thermal stability, and easy functionalization [1-5]. Despite these excellent characteristics, the self-aggregation of CNTs produced as a consequence of the strong interactions between the aromatic rings, make difficult their direct application for the development of electrochemical (bio)sensors [6-9]. Therefore, CNTs have to be functionalized to minimize these inter-tube interactions and facilitate their dispersion in aqueous media. Among the different schemes [10-14], the covalent functionalization of CNTs has demonstrated to be an interesting alternative [15, 16]. We have recently reported the development of electrochemical (bio)sensors based on the modification of glassy carbon electrode (GCE) with single-walled carbon nanotubes (SWCNT) covalently functionalized with polylysine [17] and graphene oxide nanoribbons covalently modified with polytyrosine [18].

In this work we report the synthesis and characterization of SWCNT covalently functionalized with L-Lysine (Lys) and the analytical application of GCE modified with the resulting SWCNT-Lys dispersion (GCE/SWCNT-Lys) for the highly sensitive quantification of guanine, adenine and 8-hydroxy-2´-deoxyguanosine (8OH-dG).

Guanine and adenine are important bioanalytes since they are the building blocks of DNA and RNA. Abnormal concentrations of these compounds are connected with several diseases like epilepsy, mental retardation, acquired immune deficiency syndrome (AIDS), and cancer [19]. Therefore, the development of sensitive and selective methodologies for their quantification are very important not only to understand basic aspects of DNA damage, hybridization and protein-DNA interaction [20, 21] but also in Physiology and Clinical Pathology [22]. Several methodologies have been reported for the quantification of guanine and adenine involving chromatographic [23-26] and spectrometric [27, 28] methods. However, although these techniques offer high sensitivity and selectivity, they present some disadvantages like complex sample preparation, use of sophisticated instruments, and requirement of skilled personnel that restrict their routine use.

Electrochemical methods have demonstrated to be an important alternative due to their simplicity, relative low cost, sensitivity, possibility of miniaturization and descentralized work [29]. Svorc and Kalcher [30] have reported an interesting approach for the simultaneous quantification of adenine and guanine at

a INFIQC. Departamento de Físico Química. Facultad de Ciencias Químicas. Universidad Nacional de Córdoba. Ciudad Universitaria. 5000 Córdoba, Argentina.

b *Instituto de Carboquímica (CSIC), C/ Miguel Luesma Castán 4, E-50018 Zaragoza,Spain.*
c *Current address, MSOC-Nanochemistry Group, Faculty of Chemistry, Universidad de Castilla-La Mancha. Avda. Camilo José Cela S/N, 13071, Ciudad Real (Spain).*

View Article Online
DOI: 10.1039/C5RA22556F

boron-doped diamond with detection limits at the nanomolar level. Zhou et al. [31] have proposed a very sensitive wall-jet/thin-layer glassy carbon amperometric detector coupled to high-performance liquid chromatography (HPLC) for simultaneous determination of guanine and adenine. Shpigun et al. [32] have reported the successful use of an activated carbositall electrode for the detection of purine nucleobases and related compounds by sequential injection-adsorptive stripping voltammetry. Ren et al. [33] have described the use of mesoporous carbon fiber for the simultaneous detection of the four DNA bases with a remarkably electrocatalytic activity towards both purine and pyrimidine bases. The advantages of using GCE modified with graphene nanosheets dispersed in dimethylformamide have been also reported for the sensitive and selective quantification of acetaminophen, guanine and adenine [34]. Wang et al. [35] have proposed the simultaneous detection of guanine and adenine based on the electrocatalytic activity of GCE modified with graphene quantum dots and silver nanoparticles. Thangaraj et al. [36] have described a dual GCE modified with chitosan carbon nanofiber as detector for the flow injection analysis of guanine and adenine. A recent work has demonstrated the simultaneous detection of guanine, adenine, ascorbic acid, dopamine and uric acid using a GCE modified with overoxidized polyimidazol and graphene oxide [37]. The nanomolar detection of both purines using GCE modified with nickel loaded porous carbon nanofibers has been also reported [38].

8OH-dG has received increasing attention due to its importance as biomarker for DNA damage [39-41], cancer [42, 43], neurodegenerative diseases [44, 45] and diabetes [46,47]. Different methodologies have been reported for the quantification of this important bioanalyte: HPLC with electrochemical detection [48], gas chromatography [49] and HPLC [50] in tandem with mass spectrometry, and enzyme-linked immunosorbent assay (ELISA) [51]. Wang et al. [52] have reported the highly sensitive quantification of 8OH-dG using gold nanoparticles modified with an aptamer in connection with circular dicroism. Li et al. [53] have proposed the sensitive detection of 8OH-dG and 8-nitroguanosine by capillary electrophoresis with amperometric detection after solid phase extraction with detection limits in the range of ppb. Zhang et al. [54] have reported the detection of urinary 8OH-dG with capillary electrophoresis and electrochemical detection using a molecular imprinted monolythic solid phase microextraction step.

In the following sections we present the synthesis and characterization of Lys-functionalized SWCNT, the electrochemical response of GCE/SWCNT-Lys and the analytical application for the quantification of guanine, adenine and 8OHdG.

2. Experimental

2.1. Materials and reagents

Single walled carbon nanotubes (SWCNT, AP-SWNT grade) were purchased from Carbon Solutions Inc. (Riverside, California). Sodium dodecylbenzenesulfonate (SDBS), O-(benzotriazol-1-yl)-N,N,N′,N′-tetramethyluronium hexafluorophosphate (HBTU), N,N-diisopropylethylamine (EDIPA), and Nα-(tert-Butoxycarbonyl)-L-lysine (Lys-Boc-OH), hydrogen peroxide, guanine, adenine and 8-hydroxy-2´deoxyguanosine (8OH-dG), deoxyribonucleic acid, low molecular weigth from salmon sperm (dsDNA) were purchased from Sigma-Aldrich. Sodium acetate, glacial acetic and acid ascorbic acid (AA), were received from Baker. All chemicals were reagent grade and used without further purification.

A 0.200 M acetate buffer solution pH 5.00 and 0.050M phosphate buffer solution pH 7.40 were employed as supporting electrolyte. Ultrapure water (ρ = 18 MΩ cm^{-1}) from a Millipore-MilliQ system was used for preparing all the solutions. All the experiments were conducted at room temperature.

2.2. Apparatus

The electrochemical experiments were performed with an Epsilon (BAS) potentiostat. A platinum wire and Ag/AgCl, 3M NaCl (BAS, Model RE-5B) were used as counter and reference electrodes, respectively. All potentials are referred to the latter. Bare glassy carbon (GCE) and GCE modified with SWCNT-Lys (GCE/SWCNT-Lys) were used as working electrodes. A magnetic stirrer (BASi Cell stand) and a stirring bar provided the convective transport during the amperometric measurements (at 800 rpm).

Infrared spectroscopy (FTIR) measurements were performed with a Bruker Vertex 70 spectrometer. The samples were prepared with spectroscopic-grade KBr. Thermogravimetric analysis (TGA) was performed with a Setaram balance, model Setsys Evolution 16/18, under constant nitrogen flow between room temperature and 1000ºC using a heating ramp of 10 ºC min^{-1} and 50 $mLmin^{-1}$ constant nitrogen flow.

Sonication treatments were carried out with a sonicator probe VCX 130W (Sonics and Materials, Inc.) of 20 kHz frequency containing a titanium alloy microtip (3 mm diameter) or an ultrasonic bath (TESTLAB, model TB04) 40 kHz frequency and 160 W of nominal power.

Amperometric experiments were carried out in a phosphate buffer solution (0.0500 M, pH 7.40) by applying the desired potential and allowing the transient current to decay to a steady-state value prior to the addition of the analyte and subsequent current monitoring.

2.3.Synthesis of functionalized SWCNT

SWCNT were purified by air oxidation at 350^{o}C for 2h followed by a reflux in 3M HCl for 2h. An additional drastic oxidation in a 3 M H_2SO_4/HNO_3 mixture (50:50 % v/v) was performed by refluxing for 3h (the resulting nanotubes are called SWCNT-ox). Once filtered, rinsed with deionized water and over-dried, the solid was functionalized with Lys (SWCNT-Lys). In order to avoid self-peptidic condensation and to have a homogeneous and defined functionalization typology, the covalent linking of Lys to SWCNT was directed towards the ε-amine of the aminoacid. For this reason, an α-amine Boc-protected Lys derivative was used for functionalization. In a typical experiment, 100 mg of SWCNT-ox were placed in a round-bottom flask and bath sonicated for 1h in a 0.5 % w/v SDBS aqueous solution. After that, the suspension was transferred to a schlenk flask, purged with Ar under magnetic stirring, and cooled down in a water/ice bath. To activate the cCOOH residues of SWCNT-ox with benzotriazol, 300 mg of HBTU and 2mL of EDIPA were added to the sample and allowed to react for 45 min at 0^{o}C. The covalent attachment of Lys was performed through the ε-amine by addition of 200 mg of BOc-Lys-OH and further reaction for additional 48h at room temperature. A gentle continuous flow of Ar and magnetic stirring were kept along the

View Article Online
DOI: 10.1039/C5RA22556F

whole functionalization process. Upon completion, the reaction medium was inserted in a hydrated dialysis sack (Sigma Aldrich ref. D6066), tightly tied and submerged in a 5L beaker full of deionized water. The medium was allowed to dialyze for several days, with periodical replacements of the tank water every few hours. The dialyzed medium was afterwards lyophilized in a Telstar Cryodos vacumm-freeze dryer until complete dryness. The obtained SWCNT powder was used as obtained.(Scheme 1).

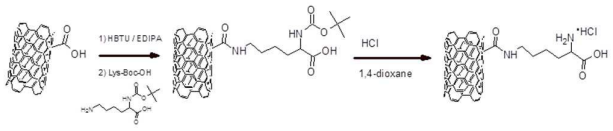

Scheme 1. Scheme of the covalent functionalization of SWCNT whit Lys.

The deprotection of the aminoacid was performed by cleaving the BOc groups that block the primary amines. The powder obtained after lyophilisation was re-dispersed in 1,4-dioxane with ultrasounds bath. After that, concentrated HCl was added to reach a final concentration of 4% v/v (HCl/dioxane), and the mixture was left at room temperature with constant magnetic stirring for 2h. Finally, it was filtered through a 0.1µm pore size Teflon membrane, rinsed with 1,4-dioxane and diethyl ether, and dried under vacuum at room temperature.

2.4. Preparation of GCE modified with SWCNT-Lys

2.4.1. Preparation of* SWCNT-Lys *dispersion: the dispersion was obtained by sonicating 1.0 mg of SWCNT-Lys with 1.0 mL 50/50 %v/v ethanol/water for 5.0 min with ultrasonic probe at 50 % amplitude. The dispersions were centrifuged for 15m at 9000rpm, and the electrodes were further modified with supernatant. The dispersions of SWCNT and SWCNT-ox in 50/50 %v/v ethanol/water were performed in a similar way.

2.4.2. Modification of GCE with SWCNT-Lys (GCE/SWCNT-Lys): GCEs were polished with alumina slurries of 1.0, 0.30, and 0.05 µm for 2 min each. Before modification with SWCNT-Lys, the electrodes were cycled in a 0.050 M phosphate buffer solution pH 7.40 for ten times between -0.300 V and 0.800 V at 0.050 Vs^{-1}. The modification was performed by depositing an aliquot of 20 µL of SWCNT-Lys on top of the GCEs followed by the evaporation of the solvent at room temperature. For comparison, GCE was also modified with dispersions of SWCNT (GCE/SWCNT) and SWCNT-ox (GCE/SWCNT-ox) in 50 % v/v in ethanol/water.

2.5. Quantification of guanine, adenine, and 8OH-dG

The quantification of guanine, adenine, and 8OH-dG was performed by voltammetric stripping analysis according to the following procedure:

(I) Preconcentration: performed at open circuit potential by immersion of GCE/SWCNT-Lys in the guanine, adenine, or 8OH-dG solution (prepared in a 0.200 M acetate buffer pH 5.00) for a given time under stirring conditions.

(II) Washing: the electrodes containing the material accumulated according to I) were washed with a 0.200 M acetate buffer solution pH 5.00 for 10 s and then transferred to a fresh acetate buffer solution.

(III) Transduction: The anodic stripping was performed in a 0.200M acetate buffer solution pH 5.00 by scanning the potential between -0.300 V and 1.500 V at 0.050 Vs^{-1} using linear scan voltammetry (LSV). The analytical signals were obtained from the oxidation peak currents of guanine, adenine, or 8OH-dG after subtracting the background currents.

All measurements were performed at room temperature.

3. Results and Discussion

3.1. Characterization of SWCNT-Lys

3.1.a. Fourier Transformed Infrared Spectroscopy (FTIR)

Figure 1A displays the FTIR spectra for SWCNT-ox and SWCNT-Lys. FTIR spectrum for SWCNT-ox shows the characteristic bands for oxygen functional groups, at 1100 cm^{-1} (C-O stretching), 1320 cm^{-1} (O-H stretching), 1722 cm^{-1} (C=O stretching) and 1580-1724 cm^{-1} overlapped signals corresponding to carboxylate, C=C aromatic stretching and O–H of adsorbed water) [55]. New bands are observed in the spectrum of SWCNT-Lys, demonstrating the success in the covalent attachment of the amino acid: 1194 cm^{-1} (secondary amine, C—N stretching), 1400 cm^{-1} (C—N stretching), 1654 cm^{-1} (amide I, C—O stretching), 1578 cm^{-1} (amide II, vibration N—H) [56]. The attached lysine also cause a pronounced increase in the intensity of Csp^3-H vibrations in methylene groups in the region between 2850 and 2950 cm^{-1}, associated with the aliphatic segments of the functional groups [55, 56].

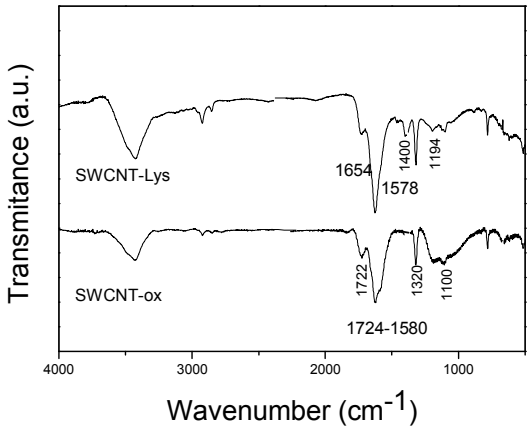

Figure 1. FT-IR spectra for: (a) SWCNT-ox, (b) SWCNT-Lys.

3.1.b.Thermogravimetric Analysis

Figure 2 shows TGA plots obtained for SWCNT (a), SWCNT-ox (b), and SWCNT-Lys (c). The slight weight loss observed for purified SWCNT indicates that they possess a very low amount of functional groups and that the oxygenated residues incorporated upon air oxidation are mostly removed during the HCl reflux [57, 58]. In the case of SWCNT-ox there is a small weight loss until 300 °C due to the release of low-stability oxygenated groups (mainly carboxylic

View Article Online
DOI: 10.1039/C5RA22556F

groups). For higher temperartures, there is an important weight loss due to the release of the additional oxygenated groups generated during the oxidation process (quinones, phenols and acid anhydrides) [57, 59].

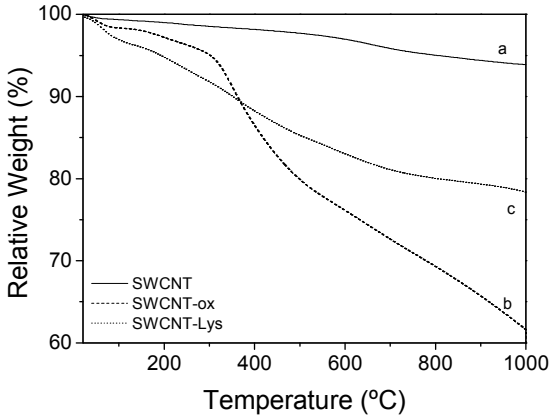

Figure 2. Thermogravimetric profiles for SWCNT (a), SWCNT-ox (b) and SWCNT-Lys (c).

The thermal stability of SWCNT-Lys is visibly higher than that of SWCNTs-ox at temperatures above 300ºC showing a gradual weight loss until 1000ºC due to the release of lysine and remaining oxygenated functional groups. Part of the oxygenated functional groups not involved in the amidation reaction are removed in the process of cleaving the BOc groups with HCl in the aminoacid deprotection [18], explaining the lower weight loss of sample SWCNT-Lys as compared to SWCNT-ox sample.

3.1.d. Cyclic voltammetry

The electrochemical behavior of GCE/SWCNT-Lys was evaluated by cyclic voltammetry using AA. Figure 3 displays cyclic voltammograms for 1.0 x 10^{-3} M AA at bare GCE (a), GCE/SWCNT-Lys (b) and GCE/SWCNT-ox (c). The comparison of both profiles clearly demonstrates that the presence of SWCNT-Lys at the glassy carbon surface produces a significant decrease in the overvoltage for AA oxidation (320 mV) as well as an increment in the capacitive currents (See also Figure 1 supplementary information). Similar experiments performed with GCE modified with a dispersion of SWCNTox (c) demonstrated that the oxidation of AA is also facilitated, although the decrease in the overvoltage is 290 mV and the current density is almost 3 times smaller than at GCE/SWCNT-Lys. Therefore, the modification of GCE with SWCNT-Lys facilitates the electrooxidation of AA due to the catalytic activity of SWCNT and the favorable interaction of AA (pKa = 4.1) with Lys residues. Similar experiments with hydrogen peroxide demonstrated a drastic decrease in the reduction and oxidation overvoltages and a substantial increment in the associated currents (not shown) at GCE/SWCNT-Lys compared to bare GCE and GCE/SWCNT-ox. These results confirm that the covalent functionalization of SWCNT makes possible an efficient dispersion of SWCNTs and the construction of a very active SWCNT-Lys modified GCE.

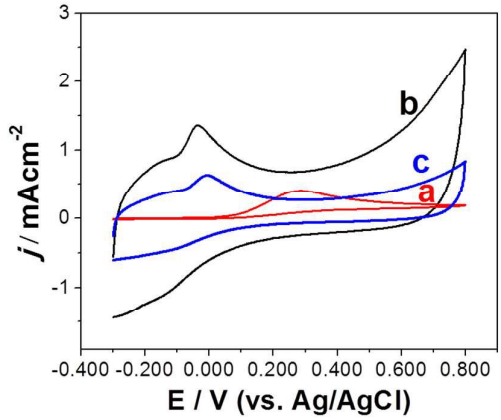

Figure 3. Cyclic voltammograms obtained at GCE (a), GCE/SWCNT-Lys (b) and GCE/SWCNT-ox for 1.0x10^{-3} M AA. Scan rate: 0.050 Vs^{-1}, supporting electrolyte: 0.050 M phosphate buffer solution pH 7.40.

3.2. Analytical applications of GCE/SWCNT-Lys for the quantification of guanine, adenine and 8-hydroxy-2´-deoxyguanosine

Figures 4A and B display linear scan voltammograms obtained in a 0.200 M acetate buffer solution after accumulation of 2.0 x 10^{-4} M guanine (A) and 2.0 x 10^{-4} M adenine (B) at bare GCE (a) and GCE/SWCNT-Lys (b) for 5.0 min at open circuit potential. At bare GCE the oxidation peak currents for guanine and adenine were 0.022 $mAcm^{-2}$ and 0.003 $mAcm^{-2}$, respectively, indicating a poor adsorption and electrooxidation after medium exchange. On the contrary, at GCE/SWCNT-Lys the peak current for guanine oxidation is 5.2 $mAcm^{-2}$ which is 236 folds higher than the one obtained at GCE. Similar behavior was observed in the case of adenine, with an oxidation peak current 697 times higher than the one obtained after adsorption and medium exchange at GCE. Is important to mention that these currents were 5.4 and 3.9 times higher than the oxidation peak currents obtained at GCE/SWCNT-Lys without accumulation for guanine and adenine, respectively (not shown). The analytical parameters for guanine electrooxidation, obtained from the calibration plot shown in Figure 4C, are the following: sensitivity of 1.1 x 10^{5} $mAM^{-1}cm^{-2}$, linear range between 2.0 x 10^{-7} M and 2.5 x 10^{-5} M (R^2 = 0.990), and detection limit of 75 nM (taken as 3σ/S where σ is the standard deviation of the blank signal and S, the sensitivity). In the case of adenine, the sensitivity is 4.2 x 10^{4} $mAM^{-1}cm^{-2}$; the linear range goes between 6.0 x 10^{-6} M and 4.0 x 10^{-5} M (R^2 = 0.9992) and the detection limit is 195 nM (parameters obtained from the calibration plot displayed in Figure 4D). No response was observed for guanine and adenine at GCE for these concentrations ranges.

View Article Online
DOI: 10.1039/C5RA22556F

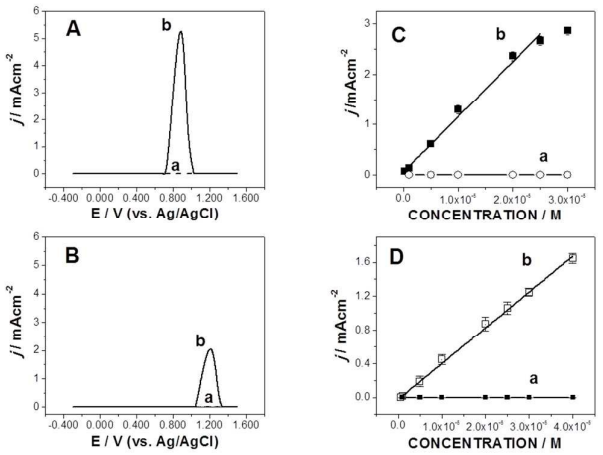

Figure 4. Linear scan voltammograms obtained in a 0.200 M acetate buffer solution pH 5.00 after accumulation for 5.0 min at open circuit potential in a 2.0 x 10^{-4} M guanine (A) and 2.0 x 10^{-4}M adenine (B) at bare GCE (a) and GCE/SWCNT-Lys (b). Calibration plots for guanine (C) and adenine (D) obtained after accumulation at open circuit potential for 5.0 min at GCE (a) and GCE/SWCNT-Lys (b). Scan rate: 0.050 Vs^{-1}; supporting electrolyte: 0.200 M acetate buffer solution pH 5.00.

Table 1 compares the analytical performance of our sensor with different guanine and adenine electrochemical sensors. Our sensor presents detection limits lower than most of those reported in Table 1 [36, 60-67]; comparable to others [68,69]; and higher than those involving hybrid materials like graphene and platinum nanoparticles [70], nickel ferrites and multi-walled carbon nanotubes [71], carboxylated graphene deposited at GCE [72] or GCE modified with polypyridinedicarboxylic acid and chemical reduced graphene oxide [73], boron doped diamond [30]. Therefore, our sensor demonstrates to be a competitive alternative for guanine and adenine quantification in a fast, simple and sensitive way.

To evaluate the analytical application of the proposed sensor we determine guanine and adenine in a salmon sperm double stranded DNA sample. Figure 5 depicts a linear scan voltammogram obtained in a 0.200 M acetate buffer solution pH 5.00 after accumulation of 200ppm dsDNA for 5.0 min and medium exchange (solid line). Two oxidation current peaks are observed at (0.828 ± 0005) V and (1.15 ± 0.02) V due to the oxidation of guanine and adenine, respectively. No signal was obtained under similar experimental conditions at bare GCE (dotted line), clearly demonstrating the advantages of the proposed sensor for further analytical applications in the field of DNA-based biosensors.

GCE/SWCNT-Lys was also used for the quantification of the important biomarker 8OH-dG. Figure 6A displays linear scan voltammograms obtained in a 0.200 M acetate buffer solution pH 5.00 after accumulation of 2.0 x 10^{-4} M 8OH-dG at GCE (a) and GCE/SWCNT-Lys (b) for 5.0 min at open circuit potential. A negligible signal is observed at bare GCE, at variance with GCE/SWCNT-Lys where a well-defined current peak of (3.8± 0.1)$mAcm^{-2}$ is obtained at (0.570 ± 0.008) V. The effect of the accumulation time of 1.0 x 10^{-5} M 8OH-dG at GCE/SWCNT-Lys at open circuit potential is displayed in Figure 6B. The oxidation peak current increases in a fast way up to 3.0 min, with a typical trend to saturation for longer times. The selected time for further analytical determinations was 5.0 min. Figure 6C depicts the calibration plot for 8OH-dG which shows a linear range between 3.0 x 10^{-7} M and 1.0 x 10^{-5} M, with a sensitivity of 8.5 x 10^{4} $mAM^{-1}cm^{-2}$ and a detection limit of 97 nM (calculated as it was previously indicated).

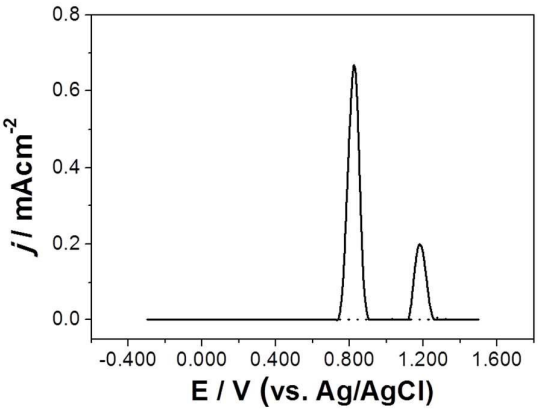

Figure 5. Linear scan voltammograms obtained in a 0.200 M acetate buffer solution pH 5.00 after accumulation for 5.0 min at open circuit potential in a 200 ppm sperm salmon double stranded DNA (dsDNA) at bare GCE (dotted line) and GCE/SWCNT-Lys (solid). Scan rate: 0.050 Vs^{-1}; supporting electrolyte: 0.200 M acetate buffer solution pH 5.00.

Taking into account the importance of detecting 8OH-dG in the presence of DNA and considering that adenine and guanine are the most easily oxidizable residues of DNA, we also evaluated the feasibility to determine 8OH-dG in the presence of adenine, guanine and dsDNA. Figure 7A depicts linear scan voltammograms obtained in a 0.200 M acetate buffer solution pH 5.00 after 5.00 min accumulation at open circuit potential of 2.0 x 10^{-5} M 8OH-dG alone (a), and in the presence of 2.0 x 10^{-4} M guanine (b) or 2.0 x 10^{-4} M adenine (c). The comparison of the different profiles indicate that a well-defined current peak for 8OH-dG oxidation is observed even in the presence of guanine and adenine at levels one-order of magnitude higher, without using any separation technique.

The detection of the oxidation of 8OH-dG in the presence of dsDNA is another important aspect considering further analytical applications of the proposed sensor. In this case, we evaluated the response of 8OH-dG in the presence of salmon sperm dsDNA.

Figure 7B displays linear scan voltammograms obtained at GCE/SWCNT-Lys in a 0.200 M acetate buffer solution pH 5.00 after 5.00 min accumulation at open circuit potential of 3.0 x 10^{-5} M 8OH-dG alone (a), and mixtures of 200 ppm dsDNA + 3.0 x 10^{-5} M 8OH-dG (b) and 200 ppm dsDNA + 2.0 x 10^{-6} M 8OH-dG (c). In the case of the mixtures dsDNA + 8OH-dG the current peaks for the oxidation of 8OH-dG can be clearly distinguished from the oxidation of the electroactive residues of dsDNA, even in the presence of 200 ppm dsDNA, demonstrating the usefulness of GCE/SWCNT-Lys for further analytical applications related to the damage of dsDNA.

View Article Online
DOI: 10.1039/C5RA22556F

Sensor	Analite	Sensitivity ($\mu A \mu M^{-1}$)	Linearity (μM)	Detection Limit (μM)	Reference
BDD electrode	G	0.082	0.21-23	0.037	30
	A	0.160	0.12-25	0.019	
β-CD-CNT/E	G	-----	1.2-20	0.20	58
	A	-----	1.0-25	0.25	
PImox-GO/GCE	G	0.421	3.3-103.3	0.48	60
	A	0.232	9.6-215	1.28	
PANI/MnO_2/GCE	G	0.1	10-240	4.8	61
	A	0.1	10-150	2.9	
CyDex-MWCNT/GCE	G	-----	100-280	33.67	62
	A	-----	4.0-20	0.75	
MWCNT–PNF–GCE	G	-----	20-3100	18.2	63
	A	-----	10-18600	8.6	
Gr–IL–CHIT–GCE	G	-----	2.5-150	0.75	64
	A	-----	1.5-350	0.45	
Gr-Naf/GCE	G	0.038	2-200	0.58	65
	A	0.077	5-200	0.75	
CoPc/CNTPEs	G	0.0149	0.6-66	0.13	66
	A	-----	-----	-----	
Chi-CNF/GCE FIA	G	0.0138	0.2-50	0.0468	67
	A	0.00484	0.2-50	0.0738	
MWCNT–CH–GCE	G	-----	0.2-450	0.06	68
	A	-----	0.4-500	0.15	
TiO_2-graphene	G	-----	0.5-200	0.1	69
	A	-----	0.5-200	0.15	
Gr-Pt hybrid NP/GCPE	G	-----	0.15-2.25	0.00112	70
	A	-----	-----	-----	
MWCNT/$NiFe_2O_4$/GCE	G	-----	0.05-3	0.006	71
	A	-----	3.0-40	0.01	
Gr-COOH/GCE	G	0.0103	0.5-200	0.050	72
	A	0.0069	0.5-200	0.025	
PDDA/CRGO/GCE	G	-----	0.05-4.5	0.01	73
	A	-----	0.1-6.0	0.02	
SWCNT-Lys/GCE	G	9.3	0.2-25	0.075	This work
	A	3.6	0.6-40	0.195	

Table 1. G: guanine; A: adenine. β-CD and CyDex: beta cyclodextrin, E: Graphite electrode, Plmox: polyimidazole -GO:graphene oxide, PANI: polyaniline, PNF: poly(new fuchsin), IL: ionic liquid, CHIT, Chi: Chitosane, Naf: Nafion, CoPc: cobalt phtalocyanine, CNTPEs: carbon nanotubes paste electrodes, CNF: carbon nanofiber, MWCNT/$NiFe_2O_4$:Multiwall carbon nanotubes/$NiFe_2O_4$ hybrid, Gr-Pt hybrid NP: graphene platinum hybrid nanoparticle,Gr-COOH: carboxilic acid functionalized graphene, BDD : Boron-doped diamond, PDDA: poly (2,6-pyridinedicarboxylic acid), CRGO: chemically reduced graphene oxide.

We have performed several controls experiments by evaluating the response of a mixture of dsDNA and 8-OHdG after accumulation and medium exchange at different electrodes: GCE, GCE/SWCNT, GCE/SWCNT-ox and GCE/SWCNT-Lys (See Table 1-Supplementary information). The comparison of the different cyclic voltammograms demonstrates that only at GCE/SWCNT-Lys is posible to simlutaneously detect the electrooxidation of guanine, adenine and 8-OHdG. The CVs obtained at GCE and GCE/SWCNT showed only the electrooxidation of guanine residues, while at GCE/SWCNT-ox the only signal was the one due to the electrooxidation of 8-OHdG, indicating that at this carboxylated surface the adsorption of the negatively charged dsDNA is very poor. These results are clear evidence of the advantages of the proposed sensor not only for the detection of dsDNA nucleobases, but also and even more important, to detect the presence of small amounts of 8-OHdG in the presence of dsDNA.

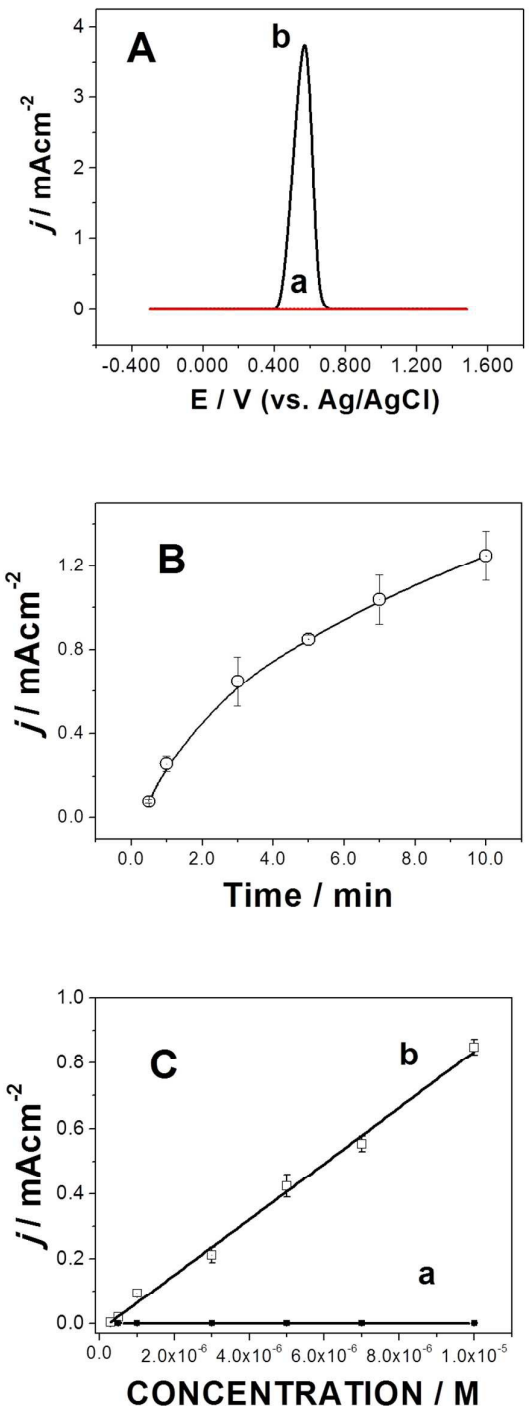

Figure 6. (A) Linear scan voltammograms obtained in a 0.200 M acetate buffer solution pH 5.00 after accumulation for 5.0 min at open circuit potential in a 2.0 x 10^{-4}M 8OH-dG at bare GCE (a) and GCE/SWCNT-Lys (b). (B) Currents obtained from linear scan voltammograms performed in a 0.200 M acetate buffer solution pH 5.00 after accumulation of 1.0 x 10^{-5} M 8OH-dG at open circuit potential for different times. (C). Calibration plot for 8OH-dG obtained from linear scan voltammograms like those showed in Figure 5A,b after accumulation of 8OH-dG at GCE/SWCNT-Lys at open circuit potential for 5.0 min. Scan rate: 0.050 Vs^{-1}; supporting electrolyte: 0.200 M acetate buffer solution pH 5.00.

View Article Online
DOI: 10.1039/C5RA22556F

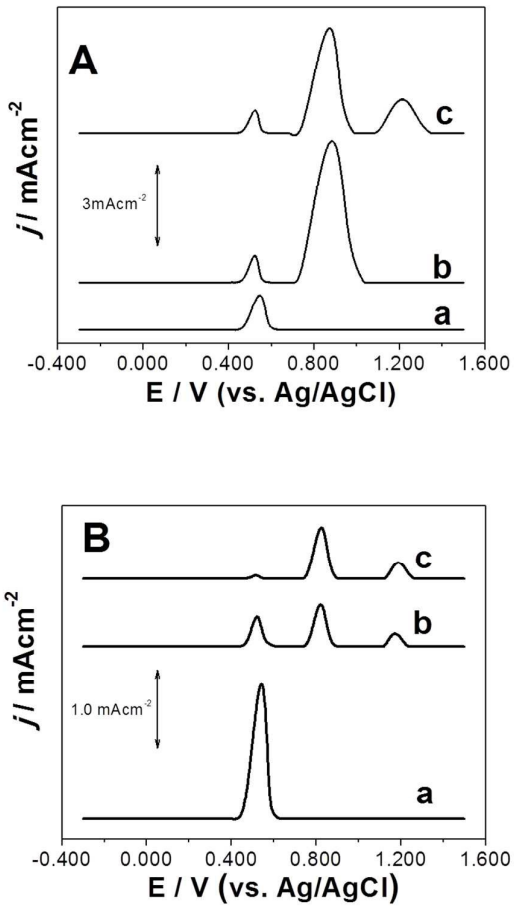

Figure 7. (A) Linear scan voltammograms obtained at GCE/SWCNT-Lys in a 0.200 M acetate buffer solution pH 5.00 after accumulation for 5.0 min at open circuit potential in: (A) 2.0 x 10^{-5} M 8OH-dG alone (a) and in the presence of 2.0 x 10^{-4} M guanine (b) or 2.0 x 10^{-4} M adenine (c); (B) 3.0 x 10^{-5} M 8OH-dG (a), 200 ppm dsDNA (b), and mixtures of 200 ppm dsDNA + 3.0 x 10^{-5} M 8OH-dG (b) and 200 ppm dsDNA + 2.0 x 10^{-6} M 8OH-dG (c) at GCE/SWCNT-Lys. Other conditions as Figure 4.

8. Conclusions

In summary, the covalent attachment of Lys to SWCNT offers an interesting alternative to efficiently disperse the nanostructures and allow a robust modification of GCE. A drastic enhancement in the sensitivity for guanine, adenine and 8OH-dG oxidation is observed at GCE/SWCNT-Lys allowing their nanomolar detection. The excellent discrimination between the oxidation signals of the electroactive residues of dsDNA and 8OH-dG at GCE/SWCNT-Lys represents a very promising alternative for future developments of DNA-damage biosensors.

Acknowledgements

The authors thank CONICET, SECyT-UNC, ANPCyT, MINCyT-Córdoba for the financial support. AG and ME thanks CONICET for the fellowship received.

References

1. Z. Wang, Z. Dai, *Nanoscale*, 2015, **7 (15)**, 6420 .
2. N. Yang, X. Chen, T. Ren, P. Zhang, D. Yang, *Sens. Actuator,* 2015, **207**, 690.
3. S. Kumar, W. Ahlawat, R. Kumar, N. Dilbaghi, *Biosens. Bioelectron*., 2015, **70**, 498.
4. P. Yáñez-Sedeño, L. Agüí, J.M. Pingarrón, *Anal. Chim. Acta*, 2014, **823**, 1.
5. M. Hasanzadeh, N. Shadjou, M. de la Guardia. *Trends Anal. Chem.*, 2015, **72**, 123.
6. A.Cernat, M. Tertiş, R. Sandulescu, F. Bedioui, A. Cristea, C. Cristea, *Anal. Chim Acta*, 2015, **886**, 16.
7. T. Fujigaya and N. Nakashima, *Sci. Technol. Adv. Mater.*, 2015, **16**, 24802.
8. J.A. Rather, s. Pilehvar and K. De Wael, *Analyst*, *2013*, **138**, 204.
9. K.C. Lin, J. Y. Huang and S.M. Chen, *RSC Adv.*, 2013, **3**, 25727.
10. E.N. Primo, F.A. Gutierrez, G.L. Luque, P.R. Dalmasso, A. Gasnier, Y. Jalit, M. Moreno, M.V. Bracamonte, M. Eguílaz Rubio, M.L. Pedano, M.C. Rodríguez, N.F. Ferreyra, M.D. Rubianes, S. Bollo, G.A. Rivas, *Anal. Chim. Acta*, 2013, **805**, 19.
11. V. Georgakilas, J. A. Perman, J. Tucek, and R. Zboril, *Chem. Rev.*, 2015, **115(11)**, 4744.
12. M.E. Ghica, C.M.A Brett, *Talanta*, 2014, 130, 198.
13. B.C. Janegitz, M. Baccarin, P.A. Raymundo-Pereira, F.A. dos Santos, G.G. Oliveira, S.A.S. Machado, M.R.V. Lanza, O. Fatibello-Filho, V. Zucolotto, *Sens. Actuators B*, 220 (2015) 805-813.
14. M.M. Barsa, M.E. Ghica, C.M.A Brett, *Anal. Chim. Acta*, 2015, **881**, 1.
15. D. Gligor and A. Walcarius, *J. Solid State Electrochem*., 2014, **18(6)**, 1519.
16. Y. Wei, X. Ling, L. Zou, D. Lai, H. Lu, Y. Xu, *Colloid Surface A*, 2015, **482**, 507.
17. A. Gasnier, J.M. González-Domínguez, A. Ansón-Casaos, J. Hernández-Ferrer, M.L. Pedano, M.D. Rubianes, M.T. Martínez and G. Rivas, *Electroanalysis*, 2014, 26, 1676.
18. J. M. González-Domínguez, F. A. Gutiérrez, J. Hernández-Ferrer, A. Ansón-Casaos, M. D. Rubianes, G. Rivas and M. T. Martínez, *J. Mater. Chem. B.*, 2015, 3, 3870.
19. Y. Wei, L. Luo, Y. Ding, X. Liu, Y. Chu, *Microchimica Acta,* 2013, **180**, 887.
20. E. M. Boon, J. E. Salas and J. K.Barton, *Nat. Biotechnol*., 2002, **20**, 282.
21. M. P. de los Santos Álvarez, J. Lobo-Castañón, J. A. Mirtanda-Ordieres, P. Tuñón-Blanco, *Electroanalysis*, 2004, **16**, 1193.
22. A. J. Li, P. McAllister, B. Y. Karlan, *Gynecol. Oncol*., 2010, **116**, 105.
23. P.C. del Moral, M.J. Arín, J.A. Resines, M.T. Diez, *J. Chromatogr. B*, 2005, **826**, 257.
24. H. Fan, F. Q. Yan, S. P. Li, *J. Pharmaceuytical Biomed. Analysis*, 2007, **45**, 141.

View Article Online
DOI: 10.1039/C5RA22556F

25. K. Kaneko, T. Yamamobe, S. Fujimori, *Biomed. Chromatogr.*, 2009, 23 () 858-864.
26. L. Liu, J. Ouyang, W. R. G. Baeyens, *J. Chromatogr. A,* 2008, **1193**, 104.
27. Y. Mei, L. Ran, H. Dongyan, G. Yuying, *Luminescence,* 2005, 20, 307.
28. D. W. Mautjana, N. A. Looi, , J. R. Eyler, A. Brajter-Toth, *Electrochim. Acta*, 2009, **55**, 52.
29. C. Zhu, G. Yang, H.Li and Y. Lin, *Anal. Chem*., 2015, **87(1)**, 230.
30. L. Švorc, K. Kalcher, *Sens. Actuator. B-Chem.*, 2014, **194**, 332.
31. Y. Zhou, H. Yan, Q. Xie, S. Yao, *Talanta*, 2015, **134**, 354.
32. L. K. Shpigun, E. Y. Andryukhina, A. S. Protasov, *J. Electroanal. Chem.*, 2015, **743**, 46.
33. S. Ren, H. Wang, H. Zhang, L. Yu, M. Li and M. Li, J. *Electroanal Chem*., 2015, **750**, 65.
34. C. Wu, Y. Tang, C. Wan, H. Liu, K. Wu, *Electrochim. Acta*, 2015, 166,285.
35. G. Wang, G. Shi, X. Chen, R. Yao, F. Chen, *Microchim. Acta*, (in press).
36. R. Thangaraj, S. Nelliapan, R. Sudhakaran, A. S. Kumar, *Electrochim. Acta*, 2014, **123**, 485.
37. X. Liu, L. Zhang, S. Wei, S. Chen, X. Ou, Q. Lu, *Biosens. Bioelectron.*, 2014, **57**, 232.
38. Y. Lu, L. Luo, Y. Ding, Y. Wang, M. Zhou, T. Zhou, D. Zhu, X. Li, *Electrochim. Acta*, 2015, **174**, 191.
39. M. S. Cooke, M. D. Evans, K. E. Herbert, J. Lunec, *Free Rad. Res.*, 2000, **32(5)**, 381.
40. H. J. Helbock, K. B. Beckman, B. N. Arnes, *Methods Enzymol*., 1999, **300**, 156.
41. S. Lofi, A. Fischer-Nielsen, J. B. Jeding, K. V. Vistisen, H. E. Poulsen, *J. Toxicol. Environ. Health*, 1993, **40**, 391.
42. H. He, Y. Zhao, N. Wang, L. Zhang, C. Wang, *Ann. Diagn. Pathol*., 2014, **18**, 326.
43. T. Dziaman, Z. Banaszkiewicz, K. Roszkowski, D. Gackowski, E. Wisniewska, R. Rozalski, M. Foksinski, A. Siomek, E. Speina, A. Winczura, A. Marszalek, B. Tudek and R. Olinski, *Int. J. Cancer*, 2014, **134**, 376.
44. S. Sharma, C. S. Moon, A. Khogali, A. Haidous, A. Chabenne, C. Ojo, M. Jelebinkov, Y. Kurdi, M. Ebadi, *Neurochem. Int*., 2013, 63, 201-229.
45. A. Valavanidis, T. Vlachogianni and C. Fiotakis, *J. Environ. Sci. Heal. C.*, 2009, 27, 120.
46. K. Broedbaek, V. Siersma, T. Henriksen, A. Weimann, M. Petersen, J. T. Andersen, E. Jimenez-Solem, L. J. Hansen, J. E. Henriksen, S. J. Bonnema, N. de F. Olivarius, S. Friis, H. E. Poulsen, *Redox Biol.*, 2015, **4**, 34.
47. K. Kotani, T. Yamada, *Singapore Med. J.*, 2014, **55(4)**, 202.
48. A. Gutiérrez, S. Osegueda, S. Gutiérrez-Granados, A. Alatorre, M. G. García and L. A Godínez, *Electroanalysis*, 2008, **20 (21)**, 2294.
49. J.-L. Ravanat, Free Rad. Research, 46(4), (2012) 479-491.
50. C.-S. Li, K.-Y. Wu, G.-P. Chang-Chien and C.C. Chou, *Environ. Sci. Technol.*, 2005, **39**, 2455.
51. R.C.S. Seet, C.-Y.J. Lee, W. M. Loke, S. H. Huang, H. Huang, W. F. Looi, E. S. Chew, A.M.L. Quek, E.C.H. Lim, B. Halliwell, *Free Radical Bio. Med.*, 2011, **50(12)**, 1787.
52. J.-C. Wang, Y.-S. Wang, J.-H. Xue, B. Zhou, Q.- M. Qian, Y. S. Wang, J.- C. Yin, H. Zhar, H. Liu, S.- D. Liu, *Biosens. Bioelectron.*, 2014, **24**, 22.
53. M.- J. Li, J.- B. Zhang, W.- L. Li, Q.- C. Chu, J. N. Ye, *J. Chromat. B.*, 2011, **879**, 3818.
54. S. Zhang, X. Song, W. Zhang, N. Luo, L. Cai, *Sci. Total Environ*, 2013, **450-451**, 266.
55. Interpretation of Infrared Spectra, A Practical Approach, John Coates in Encyclopedia of Analytical Chemistry R.A. Meyers (Ed.) pp. 10815–10837 John Wiley & Sons Ltd, Chichester, 2000.
56. C.N.R. Rao, Chemical applications of infrared spectroscopy 1963, New York and London.
57. A. Anson-Casaos, M. González, J.M. Gonzalez-Dominguez and M.T. Martínez, *Langmuir*, 2011, **27**, 7192.
58. J. M., Gonzalez-Dominguez, M. Gonzalez, A. Anson-Casaos, A. M. Diez-Pascual, M. A. Gomez, M. T. Martinez, J. Phys. Chem. C, 2011, **115(15)**, 7238.
59. P. Canete-Rosales, V. Ortega, A. Alvarez-Lueje, S. Bollo, M. Gonzalez, A. Ansón, M. T. Martinez, *Electrochim. Acta* 2012, 62, 163
60. Z. Wang, S. Xiao, Y. Chen, *J. Electroanal. Chem.*, 2006, **589**, 237.
61. X Liu,L. Zhang, S. Wei, S. Chen, X. Ou, Q. Lu, *Biosens. Bioelectron.*, 2014, **57**, 232.
62. M.U.A. Prathap, R. Srivastava, B. Satpati, *Electrochim. Acta*, 2013, **114**, 285.
63. Q. Shen, X. Wang, *J. Electroanal. Chem.*, 2009, **632**, 149.
64. C. Tang, U. Yogeswaran, S.-M. Chen, *Anal. Chim. Acta*, 2009, **636**, 19.
65. X. Niu, W. Yang, J. Ren, H. Guo, S. Long, J. Chen, J. Gao, Electrochim. Acta, 2012, **80**, 346.
66. H. Yin, Y. Zhou, Q. Ma, S. Ai, P. Ju, L. Zhu, L. Lu, *Process Biochemistry*, 2010, **45**, 1707.
67. I. Balan, I. G. David, V. David, A.-I. Stoica, C. Mihailciuc, I. Stamatin, A. A. Ciucu, *J. Electroanal. Chem.*, 2011, **654**,8.
68. P. Wang, H. Wu, Z. Dai, X. Zou, *Biosens. Bioelectron*., 2011, **26**, 3339.
69. Y. Fan, K.-J. Huang, D.-J. Niu, C.-P. Yang, Q.-S. Jing, *Electrochim. Acta*, 2011, **56**, 4685.
70. S. C. Sultan, Ü. Anik, *Talanta*, 2014, **129**, 523.
71. A. A. Ensafi, M. J.-A., B. Rezaei, A.R. Allafchian, *Sens. Actuators B. Chem.,* 2013, **177**, 634.
72. C. Li , X. Qiu, Y. Ling, *J. Electroanal. Chem.*, 2013,**704**, 44.
73. D.-H. Fan, D.-J. Niu, K.-J. Huang, *Sensor. Actuat B. Chem.,* (2008), doi:10.1016/j.snb.2010.03.023.

View Article Online
DOI: 10.1039/C5RA22556F